DOI: 10.1002/ejic.200500705

Steric and Catalytic Effects in Tetraruthenated Manganese Porphyrins

Ildemar Mayer,[a] Genebaldo S. Nunes,[a] Henrique E. Toma,[a] and Koiti Araki*[a]

Keywords: Electrochemistry / Manganese / Porphyrinoids / Sensors / Supramolecular chemistry

A new tetraruthenated manganese(III) porphyrin has been obtained and characterized by spectroscopy, electrochemistry, and spectroelectrochemistry. It exhibits a saddle-shaped, nonplanar structure that conveys interesting catalytic, electrocatalytic, and spectroelectrochemical properties to the molecule. Selective steric influence induced by the peripheral ruthenium complexes has been detected in the catalytic oxidation of cyclohexane and cyclohexene with iodosylbenzene. Films formed by layer-by-layer electrostatic assembly with tetraanionic sulfonated copper phthalocyanine exhibit electrocatalytic activity for the oxidation of nitrite and sulfite, thus providing interesting applications in amperometric sensors.

Introduction

Metalloporphyrins are an important class of molecules that are widely distributed in biological systems and play an enormous variety of roles, including catalysis, oxygen and signal transport, energy conversion, and electron transfer.[1–15] The development of new porphyrin compounds and derived materials is a subject of current research interest. New properties and functionalities can be generated by changing the molecular structure, stereochemistry, and interactions, in the context of molecular systems and materials. Particularly promising systems that exhibit remarkable catalytic and electrocatalytic properties[2,6,16–21] associated with high-valence oxygen donor species such as Mn^{V}=O[22,23] have been derived from manganese porphyrins.

Supramolecular species containing selected metal complexes attached at the periphery of the metalloporphyrin ring have been found to mimic cytochrome P-450 activity.[24] This is a consequence of the electron-withdrawing/-donating and/or electron-transfer properties of the ancillary complexes, which can also act as cofactors and create new pathways for the oxidation of organic substrates. In this sense, the understanding of their spectroscopic properties, stereochemistry, intramolecular interactions, and redox behavior is of the utmost importance.[25–29] In this work the spectroscopic and electrochemical properties of a new tetraruthenated manganese(III)porphyrin complex, [Mn(3-TRPyP)] (Figure 1), are described. Although this species can form four atropisomers, only a single configuration corresponding to a saddle geometry is inferred from molecular mechanics calculations (MM^{+}); this reflects the large steric hindrance of the peripheral bis(bipyridine)chlororuthenium(II) complexes attached at carbon 3 (*meta*) of the bridging pyridyl group (Figure 1).

The catalytic activity of [Mn(3-TRPyP)] in the oxidation of cyclohexane and cyclohexene has been investigated. In addition, the possibility to generate ultrathin supramolecular films of such species has been exploited in electrocatalysis for the oxidation of nitrite and sulfite ions in aqueous solution with the aim of generating new, efficient amperometric sensors.

Results and Discussion

Spectroscopic Properties

The insertion of Mn^{2+} ions into the free-base H_2(3-TPyP) is very fast and its oxidation to Mn^{3+} can be carried out readily in the presence of air. The resulting [Mn(3-TRPyP)] is soluble in common solvents such as methanol, ethanol, DMF, acetone, acetonitrile, and acetic acid and is sparingly soluble in water as its trifluoromethanesulfonate salt. It should be mentioned that the binding of the ruthenium complexes increases the total molecular charge to +5, thus enhancing its solubility in polar solvents. The ^{1}H NMR spectrum is complicated by the superimposition of the 2,2′-bipyridine and Mn^{III}TPyP peaks, in addition to the low molecular symmetry and to the paramagnetic character of the Mn^{III}P center. Accordingly, the structural characterization was carried out by mass spectrometry. The fragmentation profiles of the polymetalated pyridylporphyrins were found to be analogous to those previously found for the derivatives H_2(3-TRPyP) and Zn(3-TRPyP).[26,27,30,31] The peak for the [Mn(3-TRPyP)] molecular ion ($[C_{120}H_{88}Cl_4MnN_{24}Ru_4]^{5+}$ = 2467.21 g mol^{-1}) was found at *m*/*z* 494 with Δ(*m*/*z*) = 0.20 and *m*/*z* 617 with Δ(*m*/*z*) = 0.25,

[a] Instituto de Química, Universidade de São Paulo, Caixa Postal 26077, CEP 05513-970, São Paulo (SP), Brazil
E-mail: koiaraki@iq.usp.br

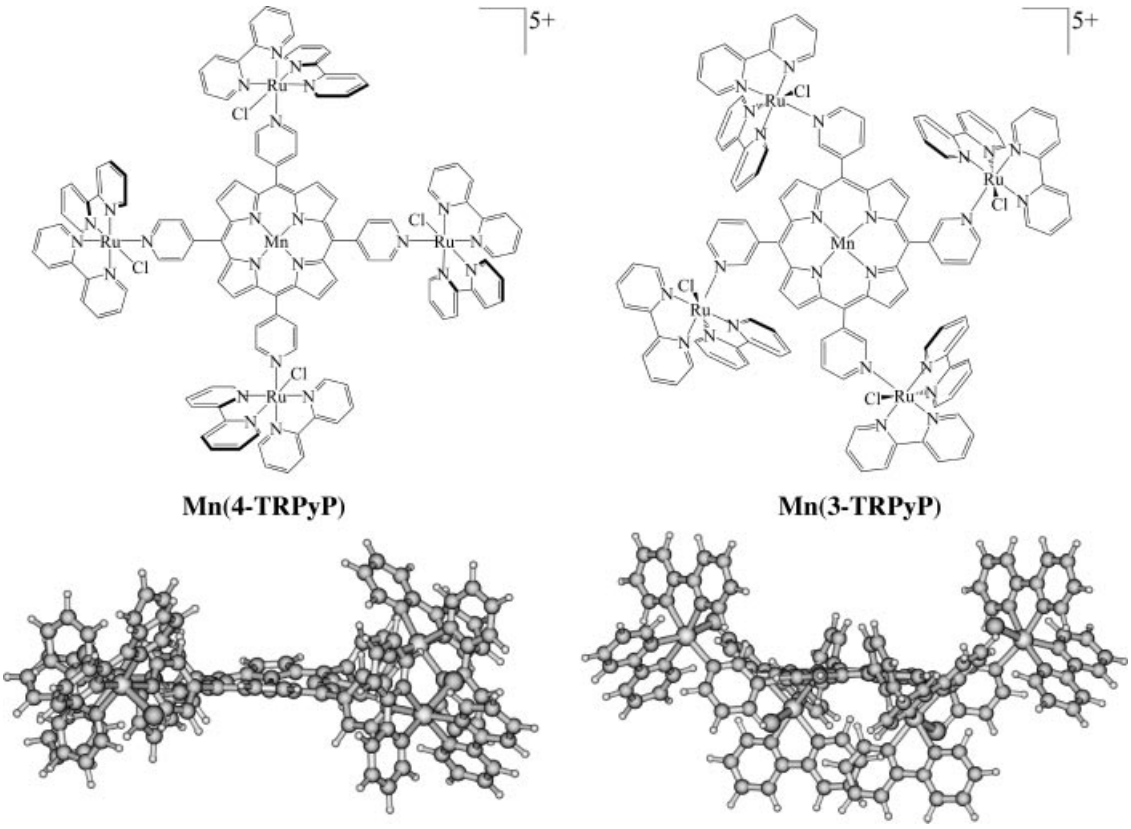

Figure 1. Structures of the tetraruthenated manganese(III) porphyrins [MnTRPyP].

suggesting the occurrence of a $Mn^{III/II}$ redox process in the spray.

[Mn(3-TRPyP)] displays a typical electronic spectrum in methanol,[32] reflecting the strong coupling between the molecular orbitals of the Mn^{III} ion and porphyrin ring.[33,34] The porphyrin bands were found at 464 nm (log ε = 5.2), attributed to the so-called band V, and 560 (4.3) and 595 nm (3.9), assigned to the IV or $Q_{(1-0)}$ and III or $Q_{(0-0)}$ porphyrin bands, respectively. The MLCT bands of the ruthenium complexes usually found at 360 and 480 nm are hidden by the bands VI (374 nm, log ε = 4.9) and V_a (399 nm, log ε = 4.9). The 2,2′-bipyridine intraligand $p\pi \rightarrow p\pi^*$ transitions of the peripheral ruthenium complexes appear at 294 nm (5.3). Finally, the Mn^{III} porphyrin bands II and I appear at 680 (1.6) and 770 nm (1.4) and are assigned to charge-transfer transitions (normally a_{1u} and $a_{2u} \rightarrow d_{xz}$ and d_{yz} transitions, respectively). They tend to become more evident when strongly coordinating ligands such as pyridine, imidazole, and pyrazine are axially coordinated.[35]

Electrochemistry

The electrochemical behavior of the polymetalated porphyrins was investigated by cyclic voltammetry and spectroelectrochemistry. The voltammograms of a solution of [Mn(3-TRPyP)] in DMF follow the general pattern previously described for the [Mn(4-TRPyP)] isomer.[32] The reversible $Ru^{III/II}$ process is observed at $E_{1/2}$ = 0.93 V (Figure 2), with a cathodic shift of 20 mV in comparison with the *para* isomer.[32] This suggests that the Mn^{III}TPyP center is acting as an electron-withdrawing group stabilizing the reduced $[Ru^{II}(bpy)_2(pyP)Cl]$ species. However, no such electronic coupling between the porphyrin ring and the peripheral ruthenium complexes is expected in the case of the *meta* isomer because of the molecular geometry. The porphyrin ring $Mn^{III}P^{+/0}$ redox process was not observed, even at potentials up to 1.50 V.

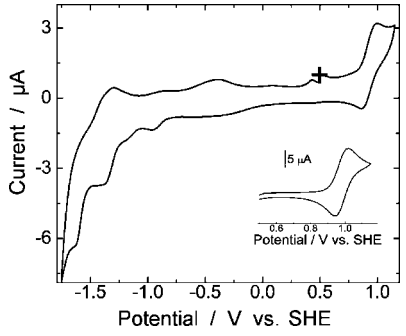

Figure 2. CV of a 2×10^{-3} M [Mn(3-TRPyP)] solution in DMF containing 0.1 M $TEAClO_4$ (scan rate: 20 mV s^{-1}).

The broad cathodic wave starting around –0.3 V was assigned to the $Mn^{III/II}P$ process and confirmed by spectroelectrochemistry. The waves at E_{pc} = –0.94 and –1.17 V can be tentatively assigned to the successive monoelectronic re-

duction of the porphyrin ring to the radical anion and dianion (Figure 2), respectively, by comparison with analogous derivatives.[11,32,36–39] However, the possibility of formation of a species with $Mn^{I}P$ character, as in the case of the respective cobalt derivative,[36–39] cannot be discarded. The single-electron reduction of one and two bipyridyl ligands of each peripheral ruthenium complex was observed at E_{pc} = –1.39 and –1.63 V, respectively. All those processes should be coupled to chemical reactions involving the solvent, and the intensity of the wave associated with the reverse anodic process is lower than for the reduction process. The anodic wave at 0.35 V can be assigned to reduced species formed in the cathodic scan because only the reversible $Ru^{III/II}$ pair of waves at $E_{1/2}$ = 0.93 V was found when the scans were limited to the 0.0 to 1.2 V range.

Spectroelectrochemistry

The spectroeletrochemical behavior of [Mn(3-TRPyP)] in DMF in the –2.2 to +1.1 V range is shown in Figure 3. The most stable form of this supramolecular complex exhibits the transition metal ions as Mn^{III} and Ru^{II} complexes. When the potential was increased from 0.5 to 1.1 V the peripheral ruthenium complex band (bpy, pπ→pπ*) at 297 nm and the MLCT bands at about 490 and 370 nm disappeared, while an absorption band rose at 316 nm. In contrast, the characteristic $Mn^{III}P$ absorption bands (III, IV, V, V_a, and VI) remained essentially unchanged. Such spectral changes (Figure 3, A) are characteristic of a reversible $Ru^{II/III}$ process, as suggested by the presence of several isosbestic points. No changes were observed in the 1.1 to 1.5 V range.

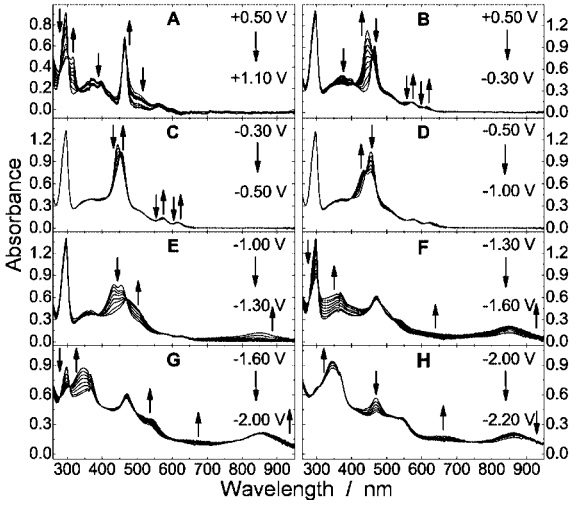

Figure 3. Spectroelectrochemistry of an approx. 80 μM solution of [Mn(3-TRPyP)] in DMF containing 0.10 M $TEAClO_4$ in the 1.1 to –2.2 V range.

The first redox process observed in the 0.5 to –0.3 V range (Figure 3, B), leads to a shift and broadening of the porphyrin Soret band from 464 to 444 nm, characteristic of the reduction of $Mn^{III}P$ to $Mn^{II}P$.[35] Interestingly, a shift of the Soret band maximum to 455 nm was observed at –0.50 V, as a function of time (Figure 3, C), giving a more symmetric and slightly less intense band. This unexpected behavior does not seem to involve a redox process and is probably associated with some axial ligand equilibrium. In this case, the participation of adventitious water molecules[5,6,32] cannot be the cause since quite negative limiting potentials (–2.2 V) could be attained.

When the potential was shifted to –1.0 V a double-peaked Soret band was formed due to the rise of a new absorption band at 433 nm and decrease of the peak at 455 nm (Figure 3, D). This behavior is not consistent with the reduction of the porphyrin ring to the respective radical anion because no characteristic band could be found around 750 nm. An equilibrium involving a face-to-face dimer is another possibility, although this doesn't involve an electron-transfer process. Accordingly, this spectroelectrochemical process was assigned to the formation of a reduced species with $Mn^{I}P$ character, as evidenced by the electrocatalytic activity of GCE modified with films of [Mn(TRPyP)]/[CuTSPc].

The reduction of the porphyrin ring was observed at –1.3 V, where a decay of the double-peaked Soret band and an increase of the absorptions at 500 and 850 nm were observed (Figure 3, E). The next two processes were observed in the ranges –1.3 to –1.6 V (Figure 3, F) and –1.6 to –2.0 V (Figure 3, G) and involve the successive decrease of the bipyridine pπ–pπ* band at 298 nm to half its value, followed by its disappearance, while a broad band rose at 350 nm. Accordingly, they were assigned to the successive single-electron reduction of the first and second bpy ligands of each peripheral ruthenium complex. Interestingly, when the potential was further shifted to –2.2 V the small peak at 470 nm associated with the porphyrin radical anion decreased as the absorbance at 660 nm increased (Figure 3, H). Those changes are typical of the formation of the porphyrin dianion. Generally, this process occurs about 200 mV after the $P^{0/-}$ process, but the reduction of the bpy ligands should shift that redox process to potentials below –2.0 V, as observed in the case of the corresponding [Co(TRPyP)] derivatives.[5,6,32,36,37]

Electrocatalytic Properties

[Mn(TRPyP)] can form stable ultrathin films of a supramolecular nanomaterial on GCE that, however, exhibit appreciable solubility in aqueous solution. This inconvenience can be eliminated by means of a layer-by-layer electrostatic assembly[32,40] with the structurally complementary tetraanionic sulfonated copper phthalocyanine [CuTSPc]. A remarkable electrochemical activity was observed for the modified electrodes (Figure 4), showing that it is possible to transfer the molecular properties of those tetraruthenated manganese porphyrins to the electrode surface. Typical CVs of GCE modified with [Mn(TRPyP)]/[CuTSPc] films in aqueous solution, at pH 4.7, exhibit a couple of reversible sine-shaped waves at $E_{1/2}$ = 0.95 V assigned to the $Ru^{III/II}$ process. The anodic and cathodic peak current intensities

increase linearly as a function of the scan rate, as expected for redox species immobilized on the surface.[9,27,40]

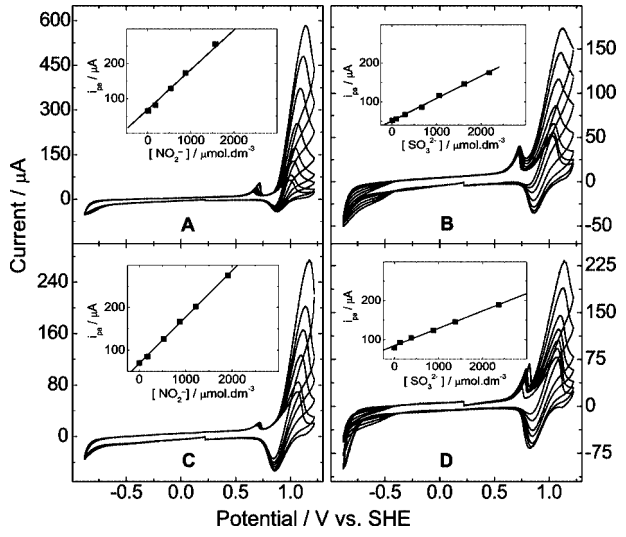

Figure 4. CVs of a GCE modified with layer-by-layer electrostatically assembled films of (A, B) [Mn(4-TRPyP)]/[CuTSPc] (Γ = 1.6 and 1.2 nmol cm^{-2}) and (C, D) [Mn(3-TRPyP)]/[CuTSPc] (Γ = 1.7 and 1.6 nmol cm^{-2}) in the presence of increasing concentrations of nitrite (A, C) and sulfite (B, D) in 0.025 M acetate buffer (pH 4.7) and KNO_3 (0.5 M). Scan rate: 0.1 V s^{-1}. Inset: plot of i_{pa} vs. [substrate].

As aliquots of a stock solution of nitrite and sulfite were added to the electrolyte solution (Figure 4) the anodic wave at 1 V intensified linearly as a function of the concentration of those species. This indicates a relatively fast heterogeneous charge-transfer process mediated by the supramolecular films, in contrast with the bare electrodes, which exhibit broad, irreproducible responses. There is no significant difference in the electrocatalytic properties of the supramolecular nanomaterials obtained with both isomers for the oxidation of sulfite and nitrite. On the other hand, both modified electrodes are ineffective for the reduction of nitrite until –0.85 V. However, this does not seem to be the case for the reduction of sulfite, for which the activity of the *meta* isomer is clearly higher. The broad reduction wave starting at –0.5 V is assigned to the reduction of sulfite directly on the GCE surface.[41,42] This contrasts with the results obtained for [Ni(TRPyP)]/[CuTSPc] and [Co(TRPyP)]/[CuTSPc] films,[43] which exhibit high activity for the reduction of both substrates. This reductive electrocatalytic activity is due to the formation of reduced species with $M^{I}P$ character, such as $Ni^{I}P$ and $Co^{I}P$, which should be responsible for the efficient electron-transfer to nitrite and sulfite. Analogously, this result for the [Mn(TRPyP)]/[CuTSPc] films reinforces our previous assignment of the spectroelectrochemistry event observed at around –1 V to the formation of a species with $Mn^{I}P$ character.

Catalytic Properties

The catalytic activity of [Mn(3-TRPyP)] species for cyclohexane hydroxylation and cyclohexene epoxidation with iodosylbenzene (PhIO) was evaluated relative to the activity of the [Mn(4-TRPyP)] isomer.[32] [Mn(3-TRPyP)] in acetonitrile solution exhibits bands V, IV, and III at 473, 574, and 616 nm, respectively. Upon adding a PhIO solution in $CH_2Cl_2/CH_3OH/H_2O$ (80:18:2) band V immediately shifts to 427 nm and bands IV and III disappear, giving rise to broad absorptions. These features are characteristic of high-valent $O{=}Mn^{IV}P$ species. However, within about a minute the spectrum of the $Mn^{III}P$ species is regenerated, indicating the consumption of PhIO and the reaction of $O{=}Mn^{IV}P$ with solvent species such as water and methanol. This suggests that the actual catalytically active species ($O{=}Mn^{V}P$) is a much more effective oxidant and oxygen atom donor (Figure 5).

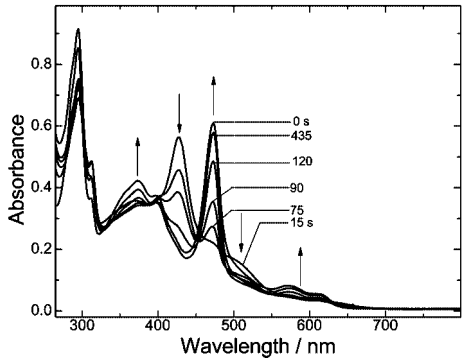

Figure 5. UV/Vis spectra showing the regeneration of $Mn^{III}P$ after reaction of a 4×10^{-6} M acetonitrile solution of [Mn(3-TRPyP)] with a PhIO solution in $CH_2Cl_2/CH_3OH/H_2O$ (80:18:2). [Mn(3-TRPyP)]:[PhIO] = 1:10.

The catalytic activity of [Mn(TRPyP)] for the oxidation of cyclohexane was verified with iodosylbenzene as oxygen donor. Typically, 9.2×10^{-4} mol of cyclohexane, 1.21×10^{-7} mol of catalyst, and 2.7×10^{-6} mol of PhIO were mixed in DCE/ACN (200/80 μL), at 298 K, in a sealed vial. The products were determined by gas chromatography after 15 min and the results are shown in Table 1. Cyclohexanol and cyclohexanone are the main products of the reaction, but small amounts of chlorocyclohexane are also observed. Interestingly, the *meta* isomer exhibits higher selectivity (alcohol/ketone ratio = 3.6 vs. 2.3) and reactivity (44% vs. 34%) than the *para* species.

More clear-cut evidence for the distinct activity of those isomers was obtained when the tetraruthenated manganese porphyrins were used as catalysts for the oxidation of cyclohexene. In general, the *meta* isomer has a significantly higher activity, converting all PhIO into oxygenated products but with a lower epoxide yield. In contrast, the *para* isomer shows a conversion of only about 60%, with a much higher selectivity for epoxide formation (Table 2).

The results described above reveal that [Mn(TRPyP)] has a catalytic activity for the oxidation of cyclohexane by PhIO similar to that of other manganese porphyrins.[44–46] For example, Iamamoto et al.[44] obtained 43% of cyclohexanol and 23% of cyclohexanone (ol/one ratio 2) with [Mn(TPP)-Cl] (chloromanganese tetraphenylporphyrin) in DCM. In general, the lower selectivity in polar solvents (for example

Table 1. Cyclohexane hydroxylation with PhIO catalyzed by tetraruthenated manganese(III) porphyrins.[a]

Catalyst	C-ol [%][c]	C-one [%][c]	C-Cl [%][c]	Ratio alcohol:ketone	Total yield [%]	TON[b]
[Mn(3-TRPyP)]	32	9	3	3.6	44	11
[Mn(4-TRPyP)]	23	10	1	2.3	34	9

[a] MnP: 1.2×10^{-7} mol; PhIO: 2.7×10^{-6} mol; cyclohexane: 9.2×10^{-4} mol; 1,2-dichloroethane (DCE): 200 μL; acetonitrile (ACN): 80 μL; chlorobenzene as internal standard; all solvents purged with N_2; T = 298 K. C-ol = cyclohexanol, C-one = cyclohexanone, C-Cl = chlorocyclohexane. [b] TON = mol products/mol catalyst. [c] Based on the initial amount of PhIO. Average error: ±3%.

Table 2. Cyclohexene oxidation with PhIO catalyzed by tetraruthenated maganese porphyrins.[a]

Catalyst	Epoxide [%][b]	C-ol [%][b]	C-one [%][b]	Allyl. oxid.	Total yield [%][b]
[Mn(3-TRPyP)]	24	40	43	0.3	107
[Mn(4-TRPyP)]	37	15	11	1	63

[a] MnP: 1.2×10^{-7} mol; PhIO: 2.7×10^{-6} mol; cyclohexene: 4.9×10^{-4} mol; 1,2-dichloroethane (DCE): 250 μL; acetonitrile (ACN): 44 μL; chlorobenzene as internal standard; all solvents purged with N_2; T = 298 K. C-ol = cyclohexen-2-ol, C-one = cyclohexen-2-one, allyl. oxid. = percentage of allylic oxidation products. [b] Based on the initial amount of PhIO. Average error ±3%.

ACN) is associated with the formation of the radical intermediate species $O{=}Mn^{IV}P^{+\cdot}$,[44,47,48] as well as the possible coordination of the solvent molecules to the Mn center. This does not seem to be the case for the [Mn(TRPyP)] complexes, however, which have a higher selectivity in DCE/ACN, in which they are more soluble because of their higher ionic character.

In the case of cyclohexane (Table 1), the higher efficiency suggests that the catalytically active high-valent oxomanganese species formed by [Mn(3-TRPyP)] is more reactive than that formed by [Mn(4-TRPyP)]. Another possibility is the involvement of two different activated species[49] as a consequence of electronic effects or interaction of the oxidant and/or the substrate with the peripheral $[Ru(bpy)_2Cl]^+$ groups. In fact, the ruthenium complexes in [Mn(3-TRPyP)] are positioned above and below the manganese porphyrin center. Accordingly, two pockets of suitable size for interaction with those organic substrates are generated, probably inducing the formation of a structurally more favorable activated complex. In contrast, the *para* isomer has a more symmetric and planar structure, ruling out such a possibility.[32]

The small amount of chlorocyclohexane (Table 1) generated in the oxidation reaction also gives some clues about the role of the peripheral ruthenium complexes in the activated complex. This by-product is likely to be formed when the cyclohexyl radical does not combine with the OH bond at the MnP center and escapes from the "cage". Consequently, its yield should be higher when the peripheral ruthenium complexes are close or interacting with the species participating in the activated complex. This proximity should facilitate the abstraction of a chloro atom from the $[Ru(bpy)_2Cl]$ groups, although the possibility of abstraction from the solvent cannot be discarded. In fact, experiments under similar conditions using another supramolecular species containing four trinuclear ruthenium acetate clusters with no coordinated chloride showed no chlorocyclohexane formation, thus ruling out the hypothesis of chlorine atom abstraction from the solvent. Considering that the redox and electronic properties of both species are similar, the significantly higher amount of chlorocyclohexane generated by the *meta* isomer is strong evidence that its higher catalytic activity can be assigned to the favorable stereochemical effects induced by the peripheral $[Ru(bipy)_2Cl]^+$ groups.

Finally, it is well known that conventional Mn–porphyrin species undergo severe degradation during the catalytic cycles,[44–48] and for this reason new, more-stable catalysts have been pursued, for example involving chlorinated or fluorinated porphyrins. In the case of the [Mn(TRPyP)] catalysts no evidence of decomposition could be detected spectroscopically after at least 10 turnover cycles, or 15 min, corresponding to the time of a typical experiment. Therefore, in spite of their secondary role in catalysis, the peripheral $[Ru(bipy)_2Cl]^+$ groups do provide an important steric protection around the highly reactive $Mn^V{=}O$ site, thereby preventing the degradation of the porphyrin center under such highly oxidizing conditions. Furthermore, they can provide interaction sites for the occurrence of steric effects, inducing changes in the geometry of the activated complex. The last two effects are probably the greatest advantage associated with these [Mn(TRPyP)] catalysts, in addition to their improved selectivity and high solubility in organic solvents.

Conclusions

A new stereochemically hindered tetraruthenated manganese(III) porphyrin has been obtained and its structural, spectroelectrochemical, catalytic, and electrocatalytic properties investigated. The metalloporphyrin reduction and ruthenium complex oxidation potentials are shifted to more negative potentials in comparison with the planar isomer, suggesting a higher electronic density on the porphyrin ring. Stable and electrocatalytically active ultrathin films of layer-by-layer electrostatic assembled films of [Mn(TRPyP)]/[CuTSPc] can be easily prepared and used as nitrite and sulfite detectors. The activity of the [Mn(3-TRPyP)]/[CuTSPc]-modified GC electrodes for the reduction of sulfite is ascribed to the formation of a reduced species with Mn^IP character at around –0.85 V, as observed by spectroelectrochemistry.

Very significant differences in the P-450 catalytic activity were found for the oxidation of cyclohexene and cyclohexane with iodosylbenzene. In fact, the *meta* isomer is consistently more active than the *para* isomer in both cases, although the selectivity for epoxide is higher for the latter. Such differences are due to steric effects induced by the peripheral [$Ru(bpy)_2Cl$] groups, which are positioned above and below the MnP ring and can therefore direct the activation of the substrates, thus improving the selectivity of the catalytic reactions. In comparison with conventional manganese porphyrins, the great advantage associated with the [Mn(TRPyP)] catalysts is their pronounced stability and improved selectivity in oxygen-transfer reactions.

Experimental Section

Materials and Methods: UV/Vis spectra were recorded with a HP-8453A diode array spectrophotometer, in the 190–1100 nm range, either in CH_3OH or CH_3CN. Cyclic voltammograms of [Mn(TRPyP)] in DMF solution were obtained with an AUTOLAB PGSTAT30 potentiostat/galvanostat. A conventional three-electrode cell was employed, consisting of a platinum disk as working electrode, Ag/Ag^+ (0.010 M, in CH_3CN) as reference electrode, and coiled platinum wire as auxiliary electrode. The solvents were HPLC grade; DMF was dried with anhydrous $CuSO_4$ and distilled under vacuum immediately before use. The electrolyte $[(C_2H_5)_4N]ClO_4$ was prepared by the reaction of $[(C_2H_5)_4N]OH$ with $HClO_4$, recrystallized from water, and dried under vacuum. A similar arrangement, except for the Ag|AgCl|KCl 1.00 M reference electrode, was used in the electrochemical studies using glassy carbon electrodes (GCE) modified with ultrathin electrostatic assembled films of [Mn(3-TRPyP)]/[CuTSPc] or [Mn(4-TRPyP)]/[CuTSPc]. All potentials were converted into the SHE scale by adding 0.503 or 0.222 V to the experimental values in organic or aqueous solution, respectively. Phosphate (25 mM, pH 6.80) and acetate (25 mM, pH 4.70) buffers in 0.50 M KNO_3 solution were used as electrolyte. The spectroelectrochemistry data were collected with a previously described homemade thin-layer cell[50] and a PAR model 173 potentiostat/galvanostat in parallel with an HP-8453A spectrophotometer. Electrospray mass spectra were recorded with a Q-Tof (Micromass) mass spectrometer with a quadrupole (Qq) and high-resolution orthogonal time of flight (o-TOF) configuration. The sample was injected with a syringe pump (Harvard Apparatus, Pump 11) at a rate of 10 $\mu L\,min^{-1}$ through an uncoated fused-silica capillary. All samples were dissolved in pure methanol. The ESI mass spectra were acquired at an ESI capillary voltage of 3 kV and a cone voltage of 10 V. Isotopic patterns were calculated using the MassLynx software. The products of the catalytic oxidation reactions were analyzed by gas chromatography using a Shimadzu model GC-17A equipment with flame ionization detector and OV-1701 0.50 micron capillary column (30 m × 0.25 mm). The carrier gas was N_2. Acetonitrile (HPLC grade) was dried over 3-Å molecular sieves before use. *n*-Octane was purified with concentrated sulfuric acid, washed with water, and distilled. Dichloromethane was distilled from over P_2O_5 and stored over molecular sieves. All other chemicals were reagent grade (1,2-dichloroethane, cyclohexane, methanol, and deuterated cyclohexane with >99% D) and used as received. Iodosylbenzene was prepared from iodobenzene diacetate as described in the literature.[51] All reactions were carried out in a thermostatted 2-mL vial with a septum, containing a magnetic stirring bar, at 25.0 ± 0.1 °C, under argon. 1,2-Dichloroethane, cyclohexane, and *n*-octane (internal reference for GC) were successively syringed into the vial, and 1.14×10^{-5} mol of PhIO was added. A suitable volume of acetonitrile stock solution of the catalyst was then introduced in order to obtain the desired concentration.

Syntheses: The preparation of the *cis*-dichlorobis(2,2′-bipyridine)-ruthenium(II) complex $[Ru(bpy)_2Cl_2]$ has been described previously.[52] [Mn(3-TPyP)] was obtained by treating 500 mg (0.80 mmol) of the free-base porphyrin H_2(3-TPyP) with 147 mg (0.85 mmol) of manganese(II) acetate in refluxing glacial acetic acid for an hour, whilst stirring. The reaction mixture was cooled to room temperature and the solvent removed in a flash evaporator. The solid was washed with water, filtered, and dried under vacuum. Yield: 97%. $C_{40}H_{24}N_8Mn(CH_3COO)\cdot H_2O$ (748.2): calcd. C 67.38, H 3.90, N 14.97; found C 67.76, H 4.12, N 15.98. [Mn(3-TRPyP)] was obtained from the reaction of 101 mg (0.15 mmol) of [Mn(3-TPyP)] with 300 mg (0.62 mmol) of $[Ru(bpy)_2Cl_2]$ in 100 mL of refluxing glacial acetic acid for an hour, whilst stirring. The solvent was removed in a flash evaporator and the residue redissolved in methanol and refluxed for 30 min to assure the coordination of four ruthenium complexes to the peripheral pyridyl nitrogen atoms. The solvent was removed, the solid redissolved in a minimum volume of DMF, and this solution added dropwise to 10 mL of an aqueous lithium trifluoromethanesulfonate solution. The brown amorphous precipitate obtained was filtered, dried under vacuum, purified by successive recrystallization, and finally by neutral alumina column chromatography using a mixture of dichloromethane and ethanol (10:1) as eluent. Yield: 89%. $C_{120}H_{88}Cl_4MnN_{24}Ru_4(CF_3SO_3)_5\cdot 8H_2O$ (3356.7): calcd. C 44.73, H 3.12, N 10.01; found C 44.52, H 3.27, N 9.49.

Acknowledgments

Financial support by FAPESP (Fundação de Amparo à Pesquisa do Estado de São Paulo), CNPq (Conselho Nacional de Desenvolvimento Científico e Tecnológico), CAPES/PICD, RENAMI (Rede de Nanomateriais Moleculares e de Interface), and the Millenium Institute of Complex Materials is gratefully acknowledged.

[1] Y. Murakami, J. Kikuchi, Y. Hisaeda, O. Hayashida, *Chem. Rev.* **1996**, *96*, 721.
[2] B. Meunier, *Chem. Rev.* **1992**, *92*, 1411.
[3] L. R. Milgrom, in *The Colours of Life: An Introduction to the Chemistry of Porphyrins and Related Compounds*, Oxford University Press, Oxford, **1997**.
[4] J. R. C. Rocha, L. Angnes, M. Bertotti, K. Araki, H. E. Toma, *Anal. Chim. Acta* **2002**, *452*, 23.
[5] S. Dovidauskas, K. Araki, H. E. Toma, *J. Porphyrins Phthalocyanines* **2000**, *4*, 727.
[6] S. Dovidauskas, H. E. Toma, K. Araki, H. C. Sacco, Y. Iamamoto, *Inorg. Chim. Acta* **2000**, *305*, 206.
[7] C. M. N. Azevedo, K. Araki, H. E. Toma, L. Angnes, *Anal. Chim. Acta* **1999**, *387*, 175.
[8] K. Araki, S. Dovidauskas, H. Winnischofer, A. D. P. Alexiou, H. E. Toma, *J. Electroanal. Chem.* **2001**, *498*, 152.
[9] K. Araki, L. Angnes, H. E. Toma, *Adv. Mater.* **1995**, *7*, 554.
[10] K. Araki, H. E. Toma, *J. Photochem. Photobiol., A* **1994**, *83*, 245.
[11] K. Araki, H. E. Toma, *J. Chem. Res. Synop.* **1994**, 290.
[12] L. Angnes, C. M. N. Azevedo, K. Araki, H. E. Toma, *Anal. Chim. Acta* **1996**, *329*, 91.
[13] L. Flamigni, A. M. Talarico, B. Ventura, G. Marconi, C. Sooambar, N. Solladie, *Eur. J. Inorg. Chem.* **2004**, 2557.
[14] E. Iengo, E. Zangrando, E. Alessio, *Eur. J. Inorg. Chem.* **2003**, 2371.
[15] J. Wojaczynski, M. Stepien, L. Latos-Grazynski, *Eur. J. Inorg. Chem.* **2002**, 1806.

[16] T. C. Zheng, D. E. Richardson, *Tetrahedron Lett.* **1995**, *36*, 833.
[17] Z. W. Tong, T. Shichi, K. Takagi, *Mater. Lett.* **2003**, *57*, 2258.
[18] Y. Naruta, M. Sasayama, *Chem. Lett.* **1994**, 2411–2414.
[19] T. J. Groves, M. K. Stern, *J. Am. Chem. Soc.* **1988**, *110*, 8628.
[20] L. Cavallo, H. Jacobsen, *Eur. J. Inorg. Chem.* **2003**, 892.
[21] E. Porhiel, A. Bondon, J. Leroy, *Eur. J. Inorg. Chem.* **2000**, 1097.
[22] N. Jin, J. T. Groves, *J. Am. Chem. Soc.* **1999**, *121*, 2923.
[23] J. T. Groves, J. Lee, S. S. Marla, *J. Am. Chem. Soc.* **1997**, *119*, 6269.
[24] B. Meunier, S. P. Visser, S. Shaik, *Chem. Rev.* **2004**, *104*, 3947.
[25] D. M. Tomazela, F. C. Gozzo, I. Mayer, F. M. Engelmann, K. Araki, H. E. Toma, M. N. Eberlin, *J. Mass Spectrom.* **2004**, *39*, 1161.
[26] I. Mayer, A. L. B. Formiga, F. M. Engelmann, H. Winnischofer, P. V. Oliveira, D. M. Tomazela, M. N. Eberlin, H. E. Toma, K. Araki, *Inorg. Chim. Acta* **2005**, *358*, 2629.
[27] I. Mayer, M. N. Eberlin, D. M. Tomazela, H. E. Toma, K. Araki, *J. Braz. Chem. Soc.* **2005**, *16*, 418.
[28] M. G. Ribeiro, G. C. Azzellini, *J. Braz. Chem. Soc.* **2003**, *14*, 914.
[29] H. E. Toma, *J. Braz. Chem. Soc.* **2003**, *14*, 845.
[30] K. Araki, H. E. Toma, *J. Coord. Chem.* **1993**, *30*, 9.
[31] H. E. Toma, K. Araki, *Coord. Chem. Rev.* **2000**, *196*, 307.
[32] K. Araki, H. Winnischofer, H. E. B. Viana, M. M. Toyama, F. M. Engelmann, I. Mayer, A. L. B. Formiga, H. E. Toma, *J. Electroanal. Chem.* **2004**, *562*, 145.
[33] S. Asher, K. Sauer, *J. Chem. Phys.* **1976**, *64*, 4115.
[34] M. Gouterman, in *The Porphyrins* (Ed.: D. Dolphin), Academic Press, New York, **1979**, vol. III, p. 347.
[35] L. J. Boucher, *Coord. Chem. Rev.* **1972**, *7*, 289.
[36] D. Sazou, C. Araullomcadams, B. C. Han, M. M. Franzen, K. M. Kadish, *J. Am. Chem. Soc.* **1990**, *112*, 7879.
[37] F. Dsouza, A. Villard, E. Vancaemelbecke, M. Franzen, T. Boschi, P. Tagliatesta, K. M. Kadish, *Inorg. Chem.* **1993**, *32*, 4042.
[38] K. Araki, L. Angnes, C. M. N. Azevedo, H. E. Toma, *J. Electroanal. Chem.* **1995**, *397*, 205.
[39] K. Araki, H. E. Toma, *Inorg. Chim. Acta* **1991**, *179*, 293.
[40] K. Araki, M. J. Wagner, M. S. Wrighton, *Langmuir* **1996**, *12*, 5393.
[41] S. M. Chen, *J. Electroanal. Chem.* **1996**, *407*, 123.
[42] S. M. Chen, S. W. Chiu, *Electrochim. Acta* **2000**, *45*, 4399.
[43] I. Mayer, H. E. Toma, K. Araki, submitted.
[44] Y. Iamamoto, M. D. Assis, K. J. Ciuffi, C. M. C. Prado, B. Z. Prellwitz, M. Moraes, O. R. Nascimento, H. C. Sacco, *J. Mol. Catal. A: Chem.* **1997**, *116*, 365.
[45] C.-C. Guo, H.-P. Li, J.-B. Xu, *J. Catal.* **1999**, *185*, 345.
[46] C.-C. Guo, J.-X. Song, X.-B. Chen, G.-F. Jiang, *J. Mol. Catal. A: Chem.* **2000**, *157*, 31.
[47] M. Gunter, P. Turner, *J. Mol. Catal.* **1991**, *66*, 121.
[48] A. Tellend, P. Bationi, D. Mansuy, *J. Chem. Soc., Chem. Commun.* **1994**, 1035.
[49] R. D. Arasasingham, G.-X. He, T. C. Bruice, *J. Am. Chem. Soc.* **1993**, *115*, 7985.
[50] H. E. Toma, K. Araki, *Curr. Org. Chem.* **2002**, *6*, 21.
[51] H. Saltzman, J. G. Sharefkin, *Org. Synth.* **1963**, *43*, 61.
[52] F. M. Engelmann, P. Losco, H. Winnischofer, K. Araki, H. E. Toma, *J. Porphyrins Phthalocyanines* **2002**, *6*, 33.

Received: August 4, 2005
Published Online: December 20, 2005

